Dopamine D2 receptor availability is linked to hippocampal–caudate functional connectivity and episodic memory

Lars Nyberg[a,b,c,1], Nina Karalija[a,c], Alireza Salami[d], Micael Andersson[b,c], Anders Wåhlin[a,c], Neda Kaboovand[d], Ylva Köhncke[d], Jan Axelsson[a,c], Anna Rieckmann[a,c], Goran Papenberg[d], Douglas D. Garrett[e,f], Katrine Riklund[a,c], Martin Lövdén[d], Ulman Lindenberger[e,f,g], and Lars Bäckman[d]

[a]Department of Radiation Sciences, Umeå University, S-901 87 Umeå, Sweden; [b]Department of Integrative Medical Biology, Umeå University, S-901 87 Umeå, Sweden; [c]Umeå Center for Functional Brain Imaging, Umeå University, S-901 87 Umeå, Sweden; [d]Aging Research Center, Karolinska Institutet, S-11330 Stockholm, Sweden; [e]Center for Lifespan Psychology, Max Planck Institute for Human Development, D-14195 Berlin, Germany; [f]Max Planck UCL Centre for Computational Psychiatry and Ageing Research, D-14195 Berlin, Germany; and [g]European University Institute, I-50014 San Domenico di Fiesole (FI), Italy

D1 and D2 dopamine receptors (D1DRs and D2DRs) may contribute differently to various aspects of memory and cognition. The D1DR system has been linked to functions supported by the prefrontal cortex. By contrast, the role of the D2DR system is less clear, although it has been hypothesized that D2DRs make a specific contribution to hippocampus-based cognitive functions. Here we present results from 181 healthy adults between 64 and 68 y of age who underwent comprehensive assessment of episodic memory, working memory, and processing speed, along with MRI and D2DR assessment with [11C]raclopride and PET. Caudate D2DR availability was positively associated with episodic memory but not with working memory or speed. Whole-brain analyses further revealed a relation between hippocampal D2DR availability and episodic memory. Hippocampal and caudate D2DR availability were interrelated, and functional MRI-based resting-state functional connectivity between the ventral caudate and medial temporal cortex increased as a function of caudate D2DR availability. Collectively, these findings indicate that D2DRs make a specific contribution to hippocampus-based cognition by influencing striatal and hippocampal regions, and their interactions.

dopamine | memory | hippocampus

Dopamine (DA) plays a key role in several cognitive processes (1–4). Reductions of D1 and D2 DA receptors (D1DRs and D2DRs) in aging (5–7) have been linked to age-related cognitive deficits (8, 9). The D1DR system has been related to functions supported by the prefrontal cortex (PFC), such as working memory and executive functions (10–12), which may reflect the relatively high density of D1DRs in the PFC (13). However, the role of D2DRs is far less clear. D2DRs are present in the PFC at very low densities (13), and evidence supporting a role for the D2DR system in working memory and executive functions is elusive (10). Pharmacological (14, 15) and PET studies assessing striatal D2DR availability (or binding potential to nondisplacable tissue uptake; BP_{ND}) with [11C]raclopride (16, 17) have yielded mixed findings in relation to cognition. It has been hypothesized that D2DRs make a specific contribution to hippocampus-based cognitive functions (10, 18, 19). Supporting these claims, positive links between D2DR BP_{ND} and episodic memory are commonly observed (20–23). PET imaging of hippocampal D2DR BP_{ND} also provides support for this hypothesis, although some studies indicate that hippocampal D2DRs may be related to both episodic memory and PFC-based executive functions (22, 23), including verbal working memory (24). Medial temporal lobe regions have been implicated in working memory (25, 26), and D2DR-mediated modulation may be exerted via hippocampal–cortical pathways (27). In addition, a [11C]raclopride task-activation PET study demonstrated contributions of striatal D2DRs to a verbal working-memory task (11).

Taken together, the specific role of the D2DR system in cognition remains unclear, likely due to the fact that past studies included small and age-heterogeneous samples and lacked comprehensive test batteries that allowed systematic comparison of the role of D2DRs in different cognitive functions. Here we present results from the Cognition, Brain, and Aging (COBRA) study that include assessment of episodic memory, working memory, and processing speed, in combination with [11C]raclopride PET and MRI of 181 healthy adults between 64 and 68 y of age (28). The main analyses concerned caudate D2DR–cognition associations, as this striatal region has been implicated in cognitive functioning (11, 12, 29, 30). Subsequently, whole-brain analyses were conducted to examine extrastriatal (especially hippocampal) D2DRs in relation to cognition. Finally, resting-state functional connectivity patterns were analyzed in relation to D2DR BP_{ND}, with special focus on interactions between the ventral caudate (31) and medial temporal cortex regions (32, 33).

Results

Caudate D2DR Availability and Cognitive Performance. We observed a significant positive relation between caudate D2DR BP_{ND} and episodic memory ($r = 0.19$, $P = 0.012$; Fig. 1A) but not for working memory or perceptual speed ($r = -0.09$, $P > 0.05$ for both). Performing the same analyses while controlling for caudate volume, correlations of similar magnitudes between D2DR BP_{ND} and performance were obtained ($r = 0.20$, $P = 0.010$ for episodic memory; $r = -0.08$, $P > 0.05$ for both working memory and speed). Thus,

Significance

Cognitive functioning depends in part on dopamine neurotransmission in the brain. Research implicates the dopamine D1 receptor family in cognitive functions linked to the prefrontal cortex, such as working memory. The dopamine D2 receptor family has also been linked to cognition, but it remains unclear to which cognitive functions it is specifically related. We examined the relation of D2 receptors to episodic memory, working memory, and speed of processing. D2 receptors in the caudate and hippocampus were related to episodic memory and modulated caudate–hippocampal functional connections. These findings link the dopamine D2 system to hippocampus-based cognitive functions.
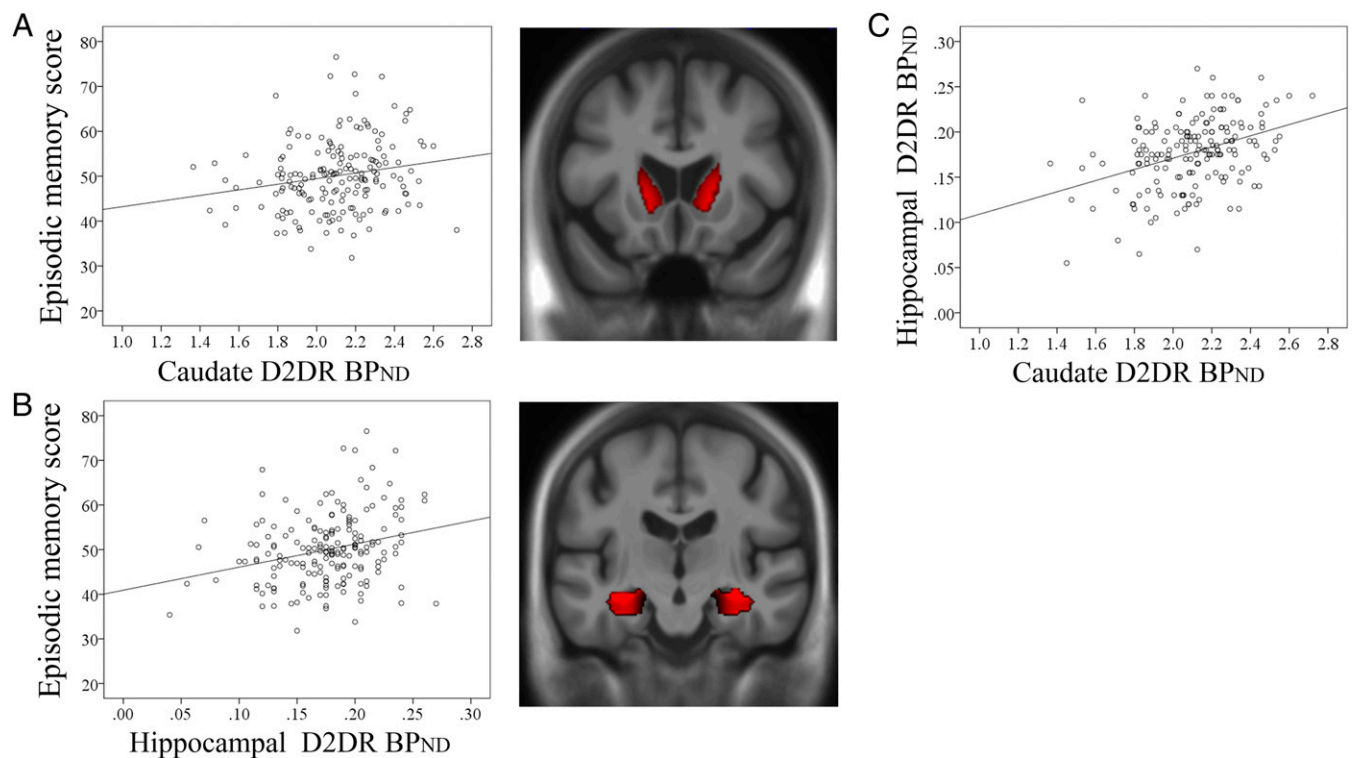
Fig. 1. Mean caudate (*A*) and hippocampal (*B*) D2DR BP$_{ND}$ correlated with episodic-memory performance, and (*C*) caudate D2DR BP$_{ND}$ was related to hippocampal D2DR BP$_{ND}$.

partial-volume effects on the D2DR BP$_{ND}$ measures were negligible (caudate D2DR BP$_{ND}$ versus volume: $r = -0.08$, $P > 0.05$). A supplementary analysis of D2DR BP$_{ND}$ in the inferior ventral caudate (*Materials and Methods*) and episodic memory confirmed a significant association ($r = 0.15$, $P = 0.05$). No correlations were found between putamen D2DR BP$_{ND}$ and cognition (all $r \leq 0.1$, $P > 0.05$), even though caudate and putamen D2DR BP$_{ND}$ were significantly interrelated ($r = 0.68$, $P < 0.001$).

Correlations between caudate D2DR BP$_{ND}$ and performance were compared with Z tests (34) for differences between cognitive abilities. The correlation between D2DR BP$_{ND}$ and episodic memory was significantly different from those for working memory ($Z = 3.23$, $P < 0.001$) and perceptual speed ($Z = 2.89$, $P = 0.002$). The corresponding correlations for working memory or perceptual speed did not differ ($Z = 0.02$, $P > 0.05$). There was no indication of quadratic associations for any of the cognitive domains ($P > 0.05$ for all domains).

Whole-Brain Voxelwise Analyses of D2DR–Cognition Associations. To assess D2DR BP$_{ND}$–cognition associations across the whole brain, cognitive-composite scores were regressed onto whole-brain D2DR BP$_{ND}$ values. The result for episodic memory revealed a significant cluster ($P < 0.05$, small-volume correction; SVC) in the left hippocampal complex ($x, y, z = -18, -10, -18$). A plot for this region revealed a positive linear association ($r = 0.30$). No significant relation was observed in the caudate, but in line with the analyses reported above, an association with episodic memory was seen in the left caudate ($x, y, z = -28, 8, 4$) at a more liberal threshold ($P < 0.01$, uncorrected). The corresponding whole-brain analyses for working memory and speed revealed no significant effects at the corrected threshold.

In view of the hippocampus finding in the whole-brain analysis, we further probed this finding with a region-of-interest (ROI) analysis, which also allowed us to consider the influence of hippocampal volume on the observed relation. Hippocampal D2DR BP$_{ND}$ values (mean 0.18; SD 0.04) were normally distributed (skewness -0.52; kurtosis 0.59) and the signal was significantly

higher than in the cerebellum [$t(180) = 67.25$, $P < 0.001$]. Critically, findings from the whole hippocampus (left and right) revealed a significant correlation with episodic memory, when controlling for hippocampal volume ($r = 0.28$, $P < 0.001$; Fig. 1*B*). A direct test of the caudate–hippocampal D2DR BP$_{ND}$ link revealed a significant positive correlation ($r = 0.38$, $P < 0.001$; Fig. 1*C*). Thus, individuals with higher caudate D2DR BP$_{ND}$ had higher hippocampal D2DR BP$_{ND}$ and higher episodic memory.

Caudate D2DR Availability in Relation to Volume and Perfusion. Caudate D2DR BP$_{ND}$ did not correlate with hippocampal, caudate, or putamen gray-matter volumes (corrected for intracranial volume; $r < 0.06$, $P > 0.05$). However, hippocampal volumes were positively correlated with episodic-memory performance ($r = 0.15$, $P = 0.04$). Furthermore, gray-matter volumes were interrelated (caudate–putamen: $r = 0.41$; caudate–hippocampus: $r = 0.24$; hippocampus–putamen: $r = 0.21$; $P < 0.01$ for all). Thus, in addition to having high D2DR BP$_{ND}$, individuals who were high-performing for episodic memory were characterized by larger hippocampal volumes. No association was found between hippocampal perfusion and D2DR BP$_{ND}$ ($r < 0.05$, $P > 0.05$).

D2DR Availability and Functional Connectivity. In light of the observed relationships of episodic memory to D2DR BP$_{ND}$ in caudate and hippocampal regions, MRI resting-state functional-connectivity data were analyzed. The functional-connectivity pattern for the inferior ventral caudate seed (VCi; *Materials and Methods*) included the bilateral hippocampus (left hippocampus: $x, y, z = -22, -20, -16$, $t = 8.93$; right hippocampus: $x, y, z = 26, -38, -2$, $t = 9.67$; Fig. 2*A*). Analyses of the relation between caudate D2DR BP$_{ND}$ and the functional connectivity map of the VCi revealed a significant positive relation in the left hippocampus/parahippocampal gyrus ($x, y, z = -22, -26, -12$; $r = 0.29$, $P = 0.05$, SVC-corrected; Fig. 2*B*) and in the left anterior medial temporal lobe (MTL; $x, y, z = -14, 2, -18$, $P = 0.005$, uncorrected). When episodic-memory performance was linked to the connectivity map of the VCi, a significant cluster was also found in an adjacent MTL region ($x, y, z = -16, 0, -10$,

$P = 0.005$, uncorrected). Given the proximity of these two MTL regions, and at the request of one reviewer, we performed a path analysis and found that the link between caudate D2DR BP$_{ND}$ and episodic memory was mediated through connectivity of the VCi and MTL (Fig. 2C). We note that this result must be interpreted with caution given the nonexperimental and cross-sectional nature of the data.

Discussion

The primary goal of this study was to examine D2DR BP$_{ND}$–cognition associations based on [11C]raclopride-PET data from a large age-homogeneous cohort of healthy adults in their mid-60s. In ROI-based analyses, we observed a positive relation of caudate and hippocampal D2DR BP$_{ND}$ to episodic memory. No associations were found between D2DR BP$_{ND}$ and working memory or perceptual speed. Thus, D2DRs appear crucial for hippocampus-based cognitive functions. Indeed, high-performing individuals were characterized by increased functional connectivity between these structures, which was positively associated with caudate D2DR BP$_{ND}$ as well as high caudate and hippocampal D2DR BP$_{ND}$ and larger hippocampal volumes.

The selective nature of the observed association for episodic memory is in line with the hypothesis that the D2DR system makes a specific contribution to hippocampus-based cognitive functions (10). This assertion is substantiated by experimental rodent work involving both genetic and pharmacological manipulations, which demonstrated that hippocampal D2DRs modulate long-term potentiation, long-term depression, as well as learning and memory (35). Further support for this hypothesis was obtained from the current whole-brain analysis. Here, an association between caudate D2DR BP$_{ND}$ and episodic memory was seen, although the strongest effects were located extrastriatally, in the hippocampal complex. This finding is consistent with observations in previous PET-imaging studies with a high-affinity D2 ligand (22, 23). Although extrastriatal D2DR availability has been detected previously with [11C]raclopride (36, 37) and with relatively high reliability (38), this low-affinity ligand is not optimal for imaging of extrastriatal BP$_{ND}$. However, the reported D2DR BP$_{ND}$ values for the hippocampus were in the expected range [5–10% of caudate levels (13)], and the signal was positive and significantly higher compared with the receptor-free cerebellar region. [11C]Raclopride binding can be influenced by blood flow (39), and individual differences in episodic memory have been related to blood-flow differences in the hippocampal region (40). Importantly, however, hippocampal perfusion was unrelated to memory performance and D2DR BP$_{ND}$.

MRI analyses of functional connectivity at rest revealed that individuals with high caudate D2DR BP$_{ND}$ and high episodic-memory scores had stronger functional interactions between the ventral caudate and hippocampus. Previous studies showed that several striatal subregions (especially caudate) and the hippocampus interact during episodic memory (41–46), and considerable overlap has been observed in the pattern of functional connectivity for hippocampal and caudate seeds (47). This suggests that these regions are part of a shared functional network. This view is further supported by meta-analytic findings of a relation between functional connectivity in the ventral caudate and hippocampus, which guided our choice of seed region (31). Animal studies have demonstrated pathways interconnecting the hippocampus and ventral striatum (48), and increased striatal DA release upon hippocampal hyperactivity (49). Past research has linked striatal DA to functional brain activity in specific brain regions in both rodents (50, 51) and humans (52–54). The present data extend these observations to the level of functional connectivity.

The results of the path analysis indicated that the association between D2DR BP$_{ND}$ and episodic memory was mediated through functional connectivity between the VCi and MTL. That is, the direct link between D2DR BP$_{ND}$ and episodic memory observed at the zero-order level was no longer reliably different from zero when the indirect link through VCi–MTL connectivity was included in the model. Given the cross-sectional, nonexperimental nature of the data, the statistical assumptions of causal mediation, such as sequential ignorability, are unlikely to be met. Hence, the mediating role of functional VCi–MTL connectivity awaits validation by longitudinal data, and the reported path coefficient must not be interpreted causally. Nevertheless, the fact that caudate D2DR BP$_{ND}$ was associated with VCi–MTL connectivity, which, in turn, had a bearing on episodic memory, extends past observations of a link among dopamine activity, functional brain activity, and memory performance (52–55) to VCi–MTL connectivity. The ventral striatum has been assigned a role in episodic memory by integrating inputs from several areas, including MTL regions (56). MTL input to the ventral striatum can affect dopaminergic activity in the ventral tegmental area (VTA). This leaves open the possibility that the observed DA–episodic memory relation is driven by stronger functional MTL input to the caudate for some individuals. On this view, MTL–VCi functional connectivity could be seen as a predictor of individual differences in episodic memory, which is in line with recent evidence that resting-state connectivity is a relatively stable individual-difference variable (57). The current findings suggest that D2DR neurotransmission contributes to this link.

Another interesting finding was that D2DR BP$_{ND}$ in the caudate and hippocampus was not only related to episodic memory but also positively interrelated. Because the caudate and hippocampus are target areas for DA projections originating from different nuclei (substantia nigra and VTA, respectively), it is in keeping with the
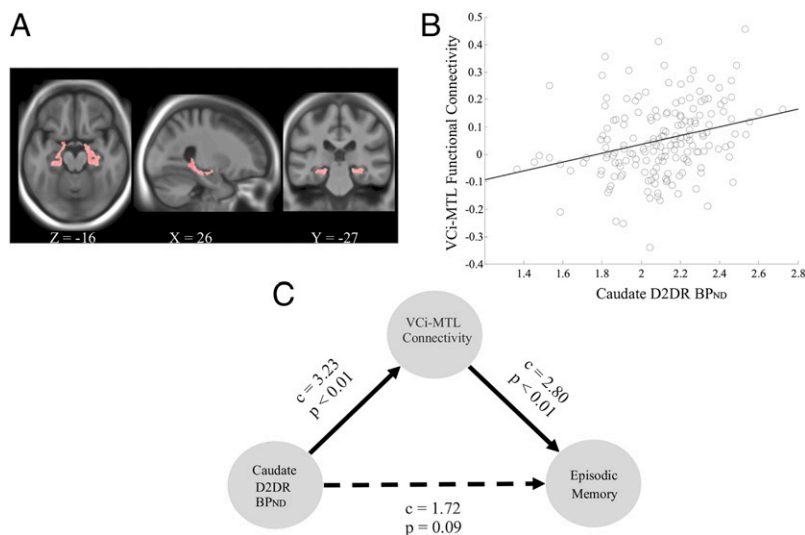

Fig. 2. (A) Horizontal, sagittal, and coronal slices showing that the functional connectivity pattern of the inferior ventral caudate included the bilateral hippocampus ($P < 0.05$, familywise error-corrected). (B) The degree of functional connectivity between the VCi and MTL was positively associated with caudate D2DR BP$_{ND}$. (C) Path analysis showing that the link between caudate D2DR BP$_{ND}$ and episodic memory was mediated through functional connectivity between the VCi and MTL. c, coefficient. Both the total and indirect effects were significant ($P < 0.05$), whereas the direct effect (dashed line) was not.

Nyberg et al.

notion that there is crosstalk between different DA pathways (58, 59) and resembles findings on D1DR BP$_{ND}$ across the major dopaminergic pathways (60). DA integrity and hippocampal volume may both be indicators of brain maintenance in aging (61, 62), a role that seems to persist when resources move toward the lower end of the distribution, as illustrated in a study of Parkinson's disease (63). D2DRs may exert protective effects against aging-related processes, such as neuroinflammation (64) and excitotoxicity in hippocampal neurons (65–70). Excitotoxicity is particularly detrimental for hippocampal neurons, possibly due to the high density of glutamatergic synapses (71–73). Relatedly, hippocampal/temporal lobe D2DRs are reduced in pathological conditions such as Alzheimer's disease, and are correlated with cognitive deficits in these patients (74–76).

The analyses of caudate D2DR–cognition associations revealed no reliable link to working memory or speed. The lack of a significant association between striatal D2DRs and working memory is noteworthy. Although this negative finding does not rule out a role of D2DRs in phasic working-memory processes (77, 78) that may require PET activation study designs to be detected (11), it suggests that basal levels of striatal D2DR do not account for between-person differences in working memory. Instead, integrity of the D1DR system (especially tonic processes therein) may be critical to performance when maintenance of information in working memory is required (27, 79, 80). Although speed of processing has been linked to DA in past theoretical (81) and empirical (20) work, reasons for the lack of association in our study could be the age homogeneity of the current sample, or that the comparison tasks we used may have taxed motor processing to a lesser degree than in previous studies.

In conclusion, our PET and functional (f)MRI findings indicate that D2DRs make a specific contribution to hippocampus-based cognition by influencing caudate and hippocampal regions and their interactions. Some of the reported effects were modest, but they were observed in a highly controlled situation with atypical age homogeneity. Thus, the current results could serve as a lower bound for robust effects in the general population. More generally, these findings support and extend previous arguments (18, 19) for a relation between DA and episodic memory.

Materials and Methods

We have previously reported the COBRA design, recruitment procedure, imaging protocols, and details of the cognitive and lifestyle battery (28). Here we restrict the presentation to methodological details directly relevant to the present results. The study was approved by the local Ethical and Radiation Safety Committee of Umeå, Sweden, and all participants provided signed written informed consent prior to initiation of any testing. Written consent was also acquired for storage of blood samples at the Department of Biobank Research at Norrland's University Hospital.

Participants. The initial sample included 181 healthy older individuals (64–68 y; mean 66.2; SD 1.2; 81 women) who were randomly selected from the population register of Umeå, in northern Sweden. Individuals with pathological deviations in brain and cognitive functions or circumstances that could bias task performance or obstruct imaging sessions (e.g., metal implants) were excluded. The resulting sample had a lower prevalence of hypertension than nationwide reports [33% in COBRA, ~50% nationwide (82)] and normal or slightly increased body-mass index (>30 in 14.4% of the sample), and 17.7% consumed nicotine. Caudate and putamen D2DR BP data were excluded for 7 individuals; these concerned cases with imperfect segmentation of MR images and PET/MR image coregistration ($n = 4$) and statistical outliers ($n = 3$). In addition, fMRI data were missing for 1 individual. Thus, the effective sample included 174 individuals.

Image Acquisition.

Structural MRI. A 3D fast spoiled gradient-echo sequence was used to achieve high-resolution anatomical T1-weighted images. These were collected as 176 slices, with thickness 1 mm, repetition time (TR) 8.2 ms, echo time (TE) 3.2 ms, flip angle 12°, and field of view 25 × 25 cm.

Functional MRI at resting state. Resting-state blood oxygen level-dependent scans were acquired using a T2*-weighted single-shot gradient echo-planar imaging sequence. Imaging parameters were 37 transaxial slices, slice thickness 3.4 mm, spacing 0.5 mm, TE/TR 30/2,000 ms, flip angle 80°, field of view 25 × 25 cm, and a 96 × 96 acquisition matrix. A total of 170 volumes were collected. Before data collection, 10 dummy scans were performed to allow steady-state imaging.

Perfusion. Whole-brain perfusion measurements were made with 3D pseudocontinuous arterial spin labeling acquired with background suppression and a spiral acquisition scheme. Labeling time 1.5 s, postlabeling delay time 1.5 s, field of view 24 cm, slice thickness 4 mm, and acquisition resolution eight arms by 512 data points, with three signal averages. Perfusion maps were calculated to obtain cerebral blood flow in ml·100 g^{-1}·min^{-1}.

PET image acquisition. All participants underwent a PET scan (Discovery PET/CT 690; GE Healthcare) performed during resting-state conditions following an i.v. bolus injection of 250 MBq [^{11}C]raclopride. Preceding the injection, a 5-min low-dose helical CT scan (20 mA, 120 kV, 0.8 s per revolution) was obtained for the purpose of PET attenuation correction. Following the bolus injection, a 55-min 18-frame dynamic scan was acquired. Attenuation- and decay-corrected PET images (47 slices, field of view 25 cm, 256 × 256-pixel transaxial images, voxel size 0.977 × 0.977 × 3.27 mm^3) were reconstructed with the iterative algorithm VUE Point HD-SharpIR [GE Healthcare (83); 6 iterations, 24 subsets, 3.0 mm postfiltering], yielding a full width at half maximum of 3.2 mm (84). Head movements during the imaging sessions were minimized with an individually fitted thermoplastic mask that was attached to the bed surface.

Cognitive Testing. Each cognitive ability (i.e., episodic memory, working memory, and perceptual speed) was evaluated with three separate tasks (verbal, numerical, and figural). Episodic memory was tested with word recall, number-word recall, and object-position recall; working memory was tested with letter-string updating, numerical 3-back, and spatial updating; and speed was tested with letter comparison, number comparison, and figure comparison (28). For each task, summary scores were computed across the total number of blocks or trials. These summary scores were standardized to form composites for each task (T score: mean 50; SD 10). Finally, the three T-scored measures per ability were averaged to create one summary score for each cognitive domain. Thus, episodic memory, working memory, and perceptual speed are each represented by one score. In the case of missing data (<1.2% for all variables), an average of the available observed scores was imputed into these ability measures so that these variables do not have any missing values.

Image Analyses.

Volumetric MRI analyses. Weighted MRI templates were used to delineate and segregate brain structures. Automatic segmentation was performed with FreeSurfer 5.3 software [surfer.nmr.mgh.harvard.edu (85–87)]. Voxel edit mode in Freeview was used to correct striatal volumes manually, when deemed necessary. The number of voxels within the delineated structures defined gray-matter volumes.

PET data analyses. For determining D2DR BP$_{ND}$ (88–90), T1-weighted MRI images and PET emission scans were merged. ROIs included the caudate, putamen, hippocampus, and cerebellum, which were delineated with FreeSurfer 5.3 segmentation software (85–87). In brief, the PET emission scan format was converted from DICOM to NIfTI, corrected for head movements, and then coregistered to the corresponding MRI image using Statistical Parametric Mapping software [SPM8 (91)]. Time–activity curves for striatal and hippocampal regions and the cerebellum were used to calculate BP$_{ND}$ using the analysis in Logan et al. (90). The cerebellum was used as a reference region due to its negligible D2DR expression (92–94).

Voxelwise analyses. PET and perfusion images were nonlinearly normalized to a sample-specific group template using diffeomorphic anatomical registration using exponentiated lie algebra [DARTEL (95)]. T1-weighted images as implemented in SPM8 were affine-aligned into stereotactic space of the Montreal Neurological Institute and smoothed using an 8.0-mm full width at half maximum Gaussian filter. To assess D2DR BP$_{ND}$–cognition associations, composite cognitive scores were regressed onto whole-brain D2DR BP$_{ND}$ values. Perfusion maps were used to examine potential confounding effects in the hippocampus.

Functional connectivity. fMRI preprocessing steps were carried out using the Data Processing Assistant for Resting-State fMRI (DPARSF), which is based upon the SPM software package (96). fMRI data were first corrected for acquisition time differences between slices within each volume and then motion-corrected. A within-subject rigid registration was carried out to align functional and structural T1-weighted images. Next, the effect of physiological noise was removed by regressing out Friston's 24 parameters of a motion model (97), as well as nuisance variables such as global signal, white matter, and cerebrospinal fluid signal, along with both linear and quadratic trends. In addition, nuisance-corrected data were band pass-filtered (passband 0.01–0.1 Hz). Finally, by means of DARTEL (95), the nuisance-corrected realigned fMRI images were nonlinearly normalized to the sample-specific group template, affine-aligned into stereotactic space of the Montreal Neurological Institute, and smoothed using an 6.0-mm full width at half maximum Gaussian filter.

Previous findings have demonstrated functional coupling between striatal regions and the MTL (31, 98). To obtain a finer parcellation, the caudate was divided into subregions. To do so, Di Martino and colleagues (98) first distinguished the ventral caudate and dorsal caudate based on the Z coordinates following ref. 31. Second, the ventral caudate was further subdivided into inferior and superior regions (VCi and VCs) (99). Note that the VCi also encompasses the nucleus accumbens. Di Martino et al. showed that the VCi (relative to VCs) is more connected functionally to several regions of the limbic system, including the hippocampus and parahippocampal gyrus. As such, we followed Di Martino and colleagues' placement of a seed in the bilateral VCi (x, y, $z = \pm 9$, $+9$, -8). Then, we generated a 4-mm-diameter sphere centered on the aforementioned coordinates, and the mean time series was computed by averaging across voxels of the seed in each hemisphere.

Multiple regression analyses were carried out for each hemisphere and subject on the time series of each seed, yielding subject-specific functional connectivity maps. The functional connectivity map for each subject was taken to a second-level multiple regression analysis to delineate regions that are functionally connected to the seed. Local maxima with $P < 0.05$ (familywise error-corrected), with an extent threshold of 10 continuous voxels ($K > 10$; $2 \times 2 \times 2$ mm per voxel), were considered to be statistically significant.

Statistical Evaluation of Associations Between Brain and Cognitive Measures. Linear and quadratic correlational analyses were carried out between the caudate and putamen (mean of left + right) D2DR BP$_{ND}$ and the cognitive ability scores. Differences between correlations were compared with Z tests. Next, performance for episodic memory, speed, and working memory were used as covariates of interest in separate voxelwise whole-brain analyses of D2DR BP$_{ND}$–cognition relations. In a subsequent step, results concerning the hippocampus were controlled for by hippocampal perfusion. Furthermore, linear associations were tested among caudate, putamen, and hippocampal gray-matter volumes, D2DR BP$_{ND}$, and cognitive performance. For within-person estimates of partial-volume effects, uncorrected gray-matter volumes and BP$_{ND}$

were compared; otherwise, corrected regional volumes were used, from which the intracranial volume factor had been regressed out (100, 101).

The functional connectivity map of the VCi and D2DR BP$_{ND}$ was analyzed, and within the resulting map the association between caudate–hippocampal connectivity and caudate D2DR BP$_{ND}$ was quantified.

The alpha level was set to $P = 0.05$ for the correlational analyses (Bonferroni-corrected for three cognitive domains; $P < 0.017$). In the whole-brain SPM analyses, an SVC was applied for the caudate and hippocampus, respectively, at a threshold of $P < 0.05$.

Mediational Analysis of the Role of Striato-Hippocampal Connectivity in the Caudate D2DR BP$_{ND}$–Episodic Memory Link. To specifically assess the potentially mediating role of functional connectivity between the VCi and MTL in the association between caudate D2DR BP$_{ND}$ and episodic memory, we conducted a path analysis. In this analysis, caudate D2DR BP$_{ND}$ served as the independent variable, VCi–MTL connectivity as the mediating variable, and the composite episodic-memory score as the dependent variable. Of chief interest was whether the link between caudate D2DR BP$_{ND}$ and episodic memory would be attenuated or eliminated once the connectivity variable was entered into the model. This analysis was conducted using the Mediation toolbox (wagerlab.colorado. edu/wiki/doku.php/help/mediation/m3_mediation_fmri_toolbox). For limitations of causal mediation analysis applied to cross-sectional, nonexperimental data, see refs. 102 and 103.

1. Cools R, D'Esposito M (2011) Inverted-U-shaped dopamine actions on human working memory and cognitive control. *Biol Psychiatry* 69(12):e113–e125.
2. Arnsten AF (1997) Catecholamine regulation of the prefrontal cortex. *J Psychopharmacol* 11(2):151–162.
3. Goldman-Rakic PS (1998) The cortical dopamine system: Role in memory and cognition. *Adv Pharmacol* 42:707–711.
4. Nieoullon A (2002) Dopamine and the regulation of cognition and attention. *Prog Neurobiol* 67(1):53–83.
5. Volkow ND, et al. (1996) Measuring age-related changes in dopamine D2 receptors with ^{11}C-raclopride and ^{18}F-N-methylspiroperidol. *Psychiatry Res* 67(1):11–16.
6. Suhara T, et al. (1991) Age-related changes in human D1 dopamine receptors measured by positron emission tomography. *Psychopharmacology (Berl)* 103(1):41–45.
7. Rinne JO, Lönnberg P, Marjamäki P (1990) Age-dependent decline in human brain dopamine D1 and D2 receptors. *Brain Res* 508(2):349–352.
8. Bäckman L, Lindenberger U, Li SC, Nyberg L (2010) Linking cognitive aging to alterations in dopamine neurotransmitter functioning: Recent data and future avenues. *Neurosci Biobehav Rev* 34(5):670–677.
9. Bäckman L, Nyberg L, Lindenberger U, Li SC, Farde L (2006) The correlative triad among aging, dopamine, and cognition: Current status and future prospects. *Neurosci Biobehav Rev* 30(6):791–807.
10. Liggins JTP (2009) The roles of dopamine D1 and D2 receptors in working memory function. *MSURJ* 4(1):39–45.
11. Bäckman L, et al. (2011) Effects of working-memory training on striatal dopamine release. *Science* 333(6043):718.
12. Rieckmann A, Karlsson S, Fischer H, Bäckman L (2011) Caudate dopamine D1 receptor density is associated with individual differences in frontoparietal connectivity during working memory. *J Neurosci* 31(40):14284–14290.
13. Hall H, et al. (1994) Distribution of D1- and D2-dopamine receptors, and dopamine and its metabolites in the human brain. *Neuropsychopharmacology* 11(4):245–256.
14. Sawaguchi T, Goldman-Rakic PS (1994) The role of D1-dopamine receptor in working memory: Local injections of dopamine antagonists into the prefrontal cortex of rhesus monkeys performing an oculomotor delayed-response task. *J Neurophysiol* 71(2):515–528.
15. Müller U, von Cramon DY, Pollmann S (1998) D1- versus D2-receptor modulation of visuospatial working memory in humans. *J Neurosci* 18(7):2720–2728.
16. Karabanov A, et al. (2010) Dopamine D2 receptor density in the limbic striatum is related to implicit but not explicit movement sequence learning. *Proc Natl Acad Sci USA* 107(16):7574–7579.
17. Volkow ND, et al. (1998) Association between decline in brain dopamine activity with age and cognitive and motor impairment in healthy individuals. *Am J Psychiatry* 155(3):344–349.
18. Lisman J, Grace AA, Duzel E (2011) A neoHebbian framework for episodic memory; role of dopamine-dependent late LTP. *Trends Neurosci* 34(10):536–547.
19. Shohamy D, Adcock RA (2010) Dopamine and adaptive memory. *Trends Cogn Sci* 14(10):464–472.
20. Bäckman L, et al. (2000) Age-related cognitive deficits mediated by changes in the striatal dopamine system. *Am J Psychiatry* 157(4):635–637.
21. Cervenka S, Bäckman L, Cselényi Z, Halldin C, Farde L (2008) Associations between dopamine D2-receptor binding and cognitive performance indicate functional compartmentalization of the human striatum. *Neuroimage* 40(3):1287–1295.
22. Takahashi H, et al. (2007) Memory and frontal lobe functions; possible relations with dopamine D2 receptors in the hippocampus. *Neuroimage* 34(4):1643–1649.
23. Takahashi H, et al. (2008) Differential contributions of prefrontal and hippocampal dopamine D(1) and D(2) receptors in human cognitive functions. *J Neurosci* 28(46):12032–12038.
24. Aalto S, Brück A, Laine M, Någren K, Rinne JO (2005) Frontal and temporal dopamine release during working memory and attention tasks in healthy humans: A positron emission tomography study using the high-affinity dopamine D2 receptor ligand [^{11}C]FLB 457. *J Neurosci* 25(10):2471–2477.
25. Axmacher N, et al. (2007) Sustained neural activity patterns during working memory in the human medial temporal lobe. *J Neurosci* 27(29):7807–7816.
26. Olson IR, Moore KS, Stark M, Chatterjee A (2006) Visual working memory is impaired when the medial temporal lobe is damaged. *J Cogn Neurosci* 18(7):1087–1097.
27. Takahashi H, Yamada M, Suhara T (2012) Functional significance of central D1 receptors in cognition: Beyond working memory. *J Cereb Blood Flow Metab* 32(7):1248–1258.
28. Nevalainen N, et al. (2015) COBRA: A prospective multimodal imaging study of dopamine, brain structure and function, and cognition. *Brain Res* 1612:83–103.
29. Dahlin E, Neely AS, Larsson A, Bäckman L, Nyberg L (2008) Transfer of learning after updating training mediated by the striatum. *Science* 320(5882):1510–1512.
30. Mendez MF, Adams NL, Lewandowski KS (1989) Neurobehavioral changes associated with caudate lesions. *Neurology* 39(3):349–354.
31. Postuma RB, Dagher A (2006) Basal ganglia functional connectivity based on a meta-analysis of 126 positron emission tomography and functional magnetic resonance imaging publications. *Cereb Cortex* 16(10):1508–1521.
32. Adcock RA, Thangavel A, Whitfield-Gabrieli S, Knutson B, Gabrieli JD (2006) Reward-motivated learning: Mesolimbic activation precedes memory formation. *Neuron* 50(3):507–517.
33. Wittmann BC, et al. (2005) Reward-related fMRI activation of dopaminergic midbrain is associated with enhanced hippocampus-dependent long-term memory formation. *Neuron* 45(3):459–467.
34. Meng X-l, Rosenthal R, Rubin DB (1992) Comparing correlated correlation coefficients. *Psychol Bull* 111(1):172–175.
35. Rocchetti J, et al. (2015) Presynaptic D2 dopamine receptors control long-term depression expression and memory processes in the temporal hippocampus. *Biol Psychiatry* 77(6):513–525.
36. Garraux G, Peigneux P, Carson RE, Hallett M (2007) Task-related interaction between basal ganglia and cortical dopamine release. *J Neurosci* 27(52):14434–14441.
37. Sawamoto N, et al. (2008) Cognitive deficits and striato-frontal dopamine release in Parkinson's disease. *Brain* 131(Pt 5):1294–1302.
38. Alakurtti K, et al. (2015) Long-term test-retest reliability of striatal and extrastriatal dopamine D2/3 receptor binding: Study with [(11)C]raclopride and high-resolution PET. *J Cereb Blood Flow Metab* 35(7):1199–1205.

39. Hassoun W, et al. (2003) PET study of the [^{11}C]raclopride binding in the striatum of the awake cat: Effects of anaesthetics and role of cerebral blood flow. *Eur J Nucl Med Mol Imaging* 30(1):141–148.
40. Nyberg L, McIntosh AR, Houle S, Nilsson LG, Tulving E (1996) Activation of medial temporal structures during episodic memory retrieval. *Nature* 380(6576):715–717.
41. Sadeh T, Shohamy D, Levy DR, Reggev N, Maril A (2011) Cooperation between the hippocampus and the striatum during episodic encoding. *J Cogn Neurosci* 23(7):1597–1608.
42. Axmacher N, Schmitz DP, Weinreich I, Elger CE, Fell J (2008) Interaction of working memory and long-term memory in the medial temporal lobe. *Cereb Cortex* 18(12):2868–2878.
43. Chua EF, Rand-Giovannetti E, Schacter DL, Albert MS, Sperling RA (2004) Dissociating confidence and accuracy: Functional magnetic resonance imaging shows origins of the subjective memory experience. *J Cogn Neurosci* 16(7):1131–1142.
44. Nichols EA, Kao YC, Verfaellie M, Gabrieli JD (2006) Working memory and long-term memory for faces: Evidence from fMRI and global amnesia for involvement of the medial temporal lobes. *Hippocampus* 16(7):604–616.
45. Prince SE, Daselaar SM, Cabeza R (2005) Neural correlates of relational memory: Successful encoding and retrieval of semantic and perceptual associations. *J Neurosci* 25(5):1203–1210.
46. Schon K, Hasselmo ME, Lopresti ML, Tricarico MD, Stern CE (2004) Persistence of parahippocampal representation in the absence of stimulus input enhances long-term encoding: A functional magnetic resonance imaging study of subsequent memory after a delayed match-to-sample task. *J Neurosci* 24(49):11088–11097.
47. Fjell AM, et al. (2016) Brain events underlying episodic memory changes in aging: A longitudinal investigation of structural and functional connectivity. *Cereb Cortex* 26(3):1272–1286.
48. Groenewegen HJ, Vermeulen-Van der Zee E, te Kortschot A, Witter MP (1987) Organization of the projections from the subiculum to the ventral striatum in the rat. A study using anterograde transport of *Phaseolus vulgaris* leucoagglutinin. *Neuroscience* 23(1):103–120.
49. Lodge DJ, Grace AA (2007) Aberrant hippocampal activity underlies the dopamine dysregulation in an animal model of schizophrenia. *J Neurosci* 27(42):11424–11430.
50. Choi J-K, Chen YI, Hamel E, Jenkins BG (2006) Brain hemodynamic changes mediated by dopamine receptors: Role of the cerebral microvasculature in dopamine-mediated neurovascular coupling. *Neuroimage* 30(3):700–712.
51. Knutson B, Gibbs SE (2007) Linking nucleus accumbens dopamine and blood oxygenation. *Psychopharmacology (Berl)* 191(3):813–822.
52. Bäckman L, et al. (2011) Dopamine D(1) receptors and age differences in brain activation during working memory. *Neurobiol Aging* 32(10):1849–1856.
53. Landau SM, Lal R, O'Neil JP, Baker S, Jagust WJ (2009) Striatal dopamine and working memory. *Cereb Cortex* 19(2):445–454.
54. Schott BH, et al. (2008) Mesolimbic functional magnetic resonance imaging activations during reward anticipation correlate with reward-related ventral striatal dopamine release. *J Neurosci* 28(52):14311–14319.
55. Nyberg L, et al. (2009) Striatal dopamine D2 binding is related to frontal BOLD response during updating of long-term memory representations. *Neuroimage* 46(4):1194–1199.
56. Pennartz CM, Ito R, Verschure PF, Battaglia FP, Robbins TW (2011) The hippocampal-striatal axis in learning, prediction and goal-directed behavior. *Trends Neurosci* 34(10):548–559.
57. Tavor I, et al. (2016) Task-free MRI predicts individual differences in brain activity during task performance. *Science* 352(6282):216–220.
58. Düzel E, et al. (2009) Functional imaging of the human dopaminergic midbrain. *Trends Neurosci* 32(6):321–328.
59. Haber SN, Knutson B (2010) The reward circuit: Linking primate anatomy and human imaging. *Neuropsychopharmacology* 35(1):4–26.
60. Rieckmann A, et al. (2011) Dopamine D1 receptor associations within and between dopaminergic pathways in younger and elderly adults: Links to cognitive performance. *Cereb Cortex* 21(9):2023–2032.
61. Lindenberger U, Burzynska AZ, Nagel IE (2013) Heterogeneity in frontal-lobe aging. *Principles of Frontal Lobe Functions*, eds Stuss DT, Knight RT (Oxford Univ Press, New York), 2nd Ed, pp 609–627.
62. Nyberg L, Lövdén M, Riklund K, Lindenberger U, Bäckman L (2012) Memory aging and brain maintenance. *Trends Cogn Sci* 16(5):292–305.
63. Jokinen P, et al. (2009) Impaired cognitive performance in Parkinson's disease is related to caudate dopaminergic hypofunction and hippocampal atrophy. *Parkinsonism Relat Disord* 15(2):88–93.
64. Shao W, et al. (2013) Suppression of neuroinflammation by astrocytic dopamine D2 receptors via αB-crystallin. *Nature* 494(7435):90–94.
65. O'Neill MJ, et al. (1998) Dopamine D2 receptor agonists protect against ischaemia-induced hippocampal neurodegeneration in global cerebral ischaemia. *Eur J Pharmacol* 352(1):37–46.
66. Vaarmann A, Kovac S, Holmström KM, Gandhi S, Abramov AY (2013) Dopamine protects neurons against glutamate-induced excitotoxicity. *Cell Death Dis* 4:e455.
67. Bozzi Y, Vallone D, Borrelli E (2000) Neuroprotective role of dopamine against hippocampal cell death. *J Neurosci* 20(22):8643–8649.
68. Coyle JT, Puttfarcken P (1993) Oxidative stress, glutamate, and neurodegenerative disorders. *Science* 262(5134):689–695.
69. Michaelis EK (1998) Molecular biology of glutamate receptors in the central nervous system and their role in excitotoxicity, oxidative stress and aging. *Prog Neurobiol* 54(4):369–415.
70. McEwen BS (2002) Sex, stress and the hippocampus: Allostasis, allostatic load and the aging process. *Neurobiol Aging* 23(5):921–939.
71. Butler TR, et al. (2010) Selective vulnerability of hippocampal cornu ammonis 1 pyramidal cells to excitotoxic insult is associated with the expression of polyamine-sensitive *N*-methyl-D-asparate-type glutamate receptors. *Neuroscience* 165(2):525–534.
72. Stoltenburg-Didinger G (1994) Neuropathology of the hippocampus and its susceptibility to neurotoxic insult. *Neurotoxicology* 15(3):445–450.
73. Walsh TJ, Emerich DF (1988) The hippocampus as a common target of neurotoxic agents. *Toxicology* 49(1):137–140.
74. Joyce JN, Myers AJ, Gurevich E (1998) Dopamine D2 receptor bands in normal human temporal cortex are absent in Alzheimer's disease. *Brain Res* 784(1–2):7–17.
75. Joyce JN, Kaeger C, Ryoo H, Goldsmith S (1993) Dopamine D2 receptors in the hippocampus and amygdala in Alzheimer's disease. *Neurosci Lett* 154(1–2):171–174.
76. Kemppainen N, et al. (2003) Hippocampal dopamine D2 receptors correlate with memory functions in Alzheimer's disease. *Eur J Neurosci* 18(1):149–154.
77. Cohen JD, Braver TS, Brown JW (2002) Computational perspectives on dopamine function in prefrontal cortex. *Curr Opin Neurobiol* 12(2):223–229.
78. Grace AA (1991) Phasic versus tonic dopamine release and the modulation of dopamine system responsivity: A hypothesis for the etiology of schizophrenia. *Neuroscience* 41(1):1–24.
79. Arnsten AF, Wang MJ, Paspalas CD (2012) Neuromodulation of thought: Flexibilities and vulnerabilities in prefrontal cortical network synapses. *Neuron* 76(1):223–239.
80. McNab F, et al. (2009) Changes in cortical dopamine D1 receptor binding associated with cognitive training. *Science* 323(5915):800–802.
81. Salthouse TA (2000) Aging and measures of processing speed. *Biol Psychol* 54(1–3):35–54.
82. Carlsson AC, Wändell PE, de Faire U, Hellénius ML (2008) Prevalence of hypertension in immigrants and Swedish-born individuals, a cross-sectional study of 60-year-old men and women in Sweden. *J Hypertens* 26(12):2295–2302.
83. Bettinardi V, et al. (2011) Physical performance of the new hybrid PET/CT Discovery-690. *Med Phys* 38(10):5394–5411.
84. Wallstén E, Axelsson J, Sundström T, Riklund K, Larsson A (2013) Subcentimeter tumor lesion delineation for high-resolution ^{18}F-FDG PET images: Optimizing correction for partial-volume effects. *J Nucl Med Technol* 41(2):85–91.
85. Fischl B, et al. (2002) Whole brain segmentation: Automated labeling of neuroanatomical structures in the human brain. *Neuron* 33(3):341–355.
86. Fischl B, et al. (2004) Sequence-independent segmentation of magnetic resonance images. *Neuroimage* 23(Suppl 1):S69–S84.
87. Han X, Fischl B (2007) Atlas renormalization for improved brain MR image segmentation across scanner platforms. *IEEE Trans Med Imaging* 26(4):479–486.
88. Mintun MA, Raichle ME, Kilbourn MR, Wooten GF, Welch MJ (1984) A quantitative model for the in vivo assessment of drug binding sites with positron emission tomography. *Ann Neurol* 15(3):217–227.
89. Innis RB, et al. (2007) Consensus nomenclature for in vivo imaging of reversibly binding radioligands. *J Cereb Blood Flow Metab* 27(9):1533–1539.
90. Logan J, et al. (1996) Distribution volume ratios without blood sampling from graphical analysis of PET data. *J Cereb Blood Flow Metab* 16(5):834–840.
91. Ashburner J, et al. (2013) *SPM8 Manual* (Wellcome Trust Centre for Neuroimaging, Institute of Neurology, University College London, London).
92. Camps M, Cortés R, Gueye B, Probst A, Palacios JM (1989) Dopamine receptors in human brain: Autoradiographic distribution of D2 sites. *Neuroscience* 28(2):275–290.
93. Farde L, Hall H, Ehrin E, Sedvall G (1986) Quantitative analysis of D2 dopamine receptor binding in the living human brain by PET. *Science* 231(4735):258–261.
94. Levey AI, et al. (1993) Localization of D1 and D2 dopamine receptors in brain with subtype-specific antibodies. *Proc Natl Acad Sci USA* 90(19):8861–8865.
95. Ashburner J (2007) A fast diffeomorphic image registration algorithm. *Neuroimage* 38(1):95–113.
96. Chao-Gan Y, Yu-Feng Z (2010) DPARSF: A MATLAB toolbox for "pipeline" data analysis of resting-state fMRI. *Front Syst Neurosci* 4:13.
97. Yan C-G, Craddock RC, He Y, Milham MP (2013) Addressing head motion dependencies for small-world topologies in functional connectomics. *Front Hum Neurosci* 7:910.
98. Di Martino A, et al. (2008) Functional connectivity of human striatum: A resting state fMRI study. *Cereb Cortex* 18(12):2735–2747.
99. Drevets WC, et al. (1999) PET measures of amphetamine-induced dopamine release in ventral versus dorsal striatum. *Neuropsychopharmacology* 21(6):694–709.
100. Jack CR, Jr, et al. (1989) Anterior temporal lobes and hippocampal formations: Normative volumetric measurements from MR images in young adults. *Radiology* 172(2):549–554.
101. Free SL, et al. (1995) Methods for normalization of hippocampal volumes measured with MR. *AJNR Am J Neuroradiol* 16(4):637–643.
102. Imai K, Keele L, Tingley D (2010) A general approach to causal mediation analysis. *Psychological Methods* 15(4):309–334.
103. Raz N, Lindenberger U (2011) Only time will tell: Cross-sectional studies offer no solution to the age-brain-cognition triangle: Comment on Salthouse (2011). *Psychol Bull* 137(5):790–795.

NEUROSCIENCE